1521-0103/347/2/398–409$25.00
THE JOURNAL OF PHARMACOLOGY AND EXPERIMENTAL THERAPEUTICS

http://dx.doi.org/10.1124/jpet.113.203976
J Pharmacol Exp Ther 347:398–409, November 2013

The Journal of PHARMACOLOGY And Experimental Therapeutics

Menthol Inhibits 5-HT_3 Receptor–Mediated Currents

Abrar Ashoor, Jacob C. Nordman, Daniel Veltri, Keun-Hang Susan Yang, Yaroslav Shuba, Lina Al Kury, Bassem Sadek, Frank C. Howarth, Amarda Shehu, Nadine Kabbani, and Murat Oz

Laboratory of Functional Lipidomics, Departments of Pharmacology (A.A., L.A.K., B.S., M.O.) and Physiology (F.C.H.), College of Medicine and Health Sciences, UAE University, Al Ain, United Arab Emirates; Department of Molecular Neuroscience (J.C.N., N.K.), School of Systems Biology (D.V.), and Department of Computer Science (A.S.), George Mason University, Fairfax, Virginia; International Center of Molecular Physiology of the National Academy of Sciences of Ukraine, Kiev, Ukraine (Y.S.); and Department of Biological Sciences, Schmid College of Science and Engineering, Chapman University, Orange, California (K.-H.S.Y.)

Received March 2, 2013; accepted July 8, 2013

ABSTRACT

The effects of alcohol monoterpene menthol, a major active ingredient of the peppermint plant, were tested on the function of human 5-hydroxytryptamine type 3 (5-HT_3) receptors expressed in *Xenopus laevis* oocytes. 5-HT (1 μM)-evoked currents recorded by two-electrode voltage-clamp technique were reversibly inhibited by menthol in a concentration-dependent (IC_{50} = 163 μM) manner. The effects of menthol developed gradually, reaching a steady-state level within 10–15 minutes and did not involve G-proteins, since GTPγS activity remained unaltered and the effect of menthol was not sensitive to pertussis toxin pretreatment. The actions of menthol were not stereoselective as (−), (+), and racemic menthol inhibited 5-HT_3 receptor–mediated currents to the same extent. Menthol inhibition was not altered by intracellular 1,2-bis(*o*-aminophenoxy)ethane-*N,N,N′,N′*-tetraacetic acid injections and transmembrane potential changes. The maximum inhibition observed for menthol was not reversed by increasing concentrations of 5-HT. Furthermore, specific binding of the 5-HT_3 antagonist [^{3}H]GR65630 was not altered in the presence of menthol (up to 1 mM), indicating that menthol acts as a noncompetitive antagonist of the 5-HT_3 receptor. Finally, 5-HT_3 receptor–mediated currents in acutely dissociated nodose ganglion neurons were also inhibited by menthol (100 μM). These data demonstrate that menthol, at pharmacologically relevant concentrations, is an allosteric inhibitor of 5-HT_3 receptors.

Introduction

Menthol is among the world's most important flavoring agents and is used in a variety of commercial products such as toothpaste, mouthwash, foods, cigarettes, and oral pharmaceutical preparations (Eccles, 1994; Patel et al., 2007). Menthol is a monocyclic terpene alcohol that occurs naturally in more than 100 essential oils, including spearmint and peppermint. The discovery of menthol activation of transient receptor potential melastatin subfamily channel 8 (TRPM8) was a major breakthrough in understanding the molecular mechanisms underlying menthol's cooling action (Jordt et al., 2003). Besides its importance in cool sensation, menthol is the major active ingredient of various herbal medicines. Since antiquity, peppermint (a major constituent of which is menthol) has been used widely for various medicinal purposes ranging from management of musculoskeletal pain and the common cold to the treatment of gastrointestinal disorders such as nausea, vomiting, and irritable bowel syndrome (for reviews, see Grigoleit and Grigoleit, 2005; Cappello et al., 2007; Patel et al., 2007; and Haniadka et al., 2012). However, the cellular and molecular targets mediating the beneficial effects of peppermint and other menthol-containing products on gastrointestinal disorders are currently unknown (De Araújo et al., 2011).

The 5-hydroxytryptamine type 3 (5-HT_3) receptor, a member of the Cys-loop family of ligand-gated ion channels, mediates fast depolarizing actions of 5-HT in the central and peripheral nervous system (Yakel and Jackson, 1988). 5-HT_3 receptors are also expressed by enteric sensory neurons in the mucosal layer and in the nerve cell body of interneurons and motor neurons in the enteric nervous system (Galligan, 2002). The peristaltic reflex can be initiated by release of 5-HT following stimulation of enterochromaffin cells by pressure or other intraluminal stimulus and subsequent stimulation through 5-HT_3 receptors of ganglionic and synaptic transmission in the myenteric plexus. Involvement of 5-HT_3 receptors in nausea, vomiting, and irritable bowel syndrome has been well established (for reviews,

This study was supported in part by the Intramural Research Program of the National Institutes of Health [National Institute on Drug Abuse]; and by UAE University research funds. Research in our laboratory is also supported by LABCO, partner of Sigma-Aldrich.
dx.doi.org/10.1124/jpet.113.203976.

ABBREVIATIONS: 5-HT, 5-hydroxytryptamine; 5-HTR, 5-HT receptor; ANOVA, analysis of variance; BAPTA, 1,2-bis(*o*-aminophenoxy)ethane-*N,N,N′,N′*-tetraacetic acid; DA, dopamine; DMSO, dimethylsulfoxide; $GABA_AR$, γ-aminobutyric acid α receptor; GR65630, 3-(5-methyl-1*H*-imidazol-4-yl)-1-(1-methylindol-3-yl)propan-1-one; LY278584, 1-methyl-*N*-(8-methyl-8-azabicyclo[3.2.1]-oct-3-yl)-1*H*-indazole-3-carboxamide; MDL72222, tropanyl 3,5-dichlorobenzoate; nAChR, nicotinic acetylcholine receptor; PMSF, phenylmethylsulfonyl fluoride, PTX, pertussis toxin; TRPM8, transient receptor potential melastatin subfamily channel 8.

see Riering et al., 2004; and Faerber et al., 2007). In fact, antagonists of the 5-HT$_3$ receptor are currently among the most effective therapeutic agents in treatment of chemotherapy-induced nausea, vomiting, and irritable bowel syndrome (for a review, see Thompson and Lummis, 2007). Interestingly, there is considerable overlap between the gastrointestinal actions of menthol and 5-HT$_3$ receptor antagonists. Therefore, it is likely that some of the actions of menthol involve modulation of 5-HT$_3$ receptor function.

In this study, using electrophysiological and biochemical methods, we have investigated the effect of menthol on the functional properties of human 5-HT$_3$ receptors expressed in *Xenopus laevis* oocytes and 5-HT$_3$ receptors of rat nodose ganglion neurons.

Materials and Methods

Mature female *X. laevis* frogs were purchased from Xenopus Express (Haute-Loire, France) and were housed in dechlorinated tap water at 18°C and fed with dry frog pellets at least twice a week. Clusters of oocytes were removed surgically under benzocaine (Sigma-Aldrich, St. Louis, MO) anesthesia [0.03% (w/v)]. Individual oocytes were manually dissected away in a solution containing 88 mM NaCl, 1 mM KCl, 2.4 mM $NaHCO_3$, 0.8 mM $MgSO_4$, and 10 mM HEPES (pH 7.5), and stored for 2–7 days in modified Barth's solution containing 88 mM NaCl, 1 mM KCl, 2.4 mM $NaHCO_3$, 2 mM $CaCl_2$, 0.8 mM $MgSO_4$. 10 mM HEPES (pH 7.5), supplemented with 2 mM sodium pyruvate, 10,000 IU/l penicillin, 10 mg/l streptomycin, 50 mg/l gentamicin, and 0.5 mM theophylline. Oocytes were placed in a 0.2-ml recording chamber and superfused at a constant rate of 3–5 ml/min. The bathing solution consisted of 95 mM NaCl, 2 mM KCl, 2 mM $CaCl_2$, and 5 mM HEPES (pH 7.5). 5-HT$_{3A}$ receptor cRNA (3 ng) was injected into each oocyte. After 2 days, cells were impaled with two standard glass microelectrodes filled with a 3 M KCl (1–3 MΩ). The oocytes were routinely voltage-clamped at a holding potential of −70 mV using GeneClamp-500B amplifier (Axon Instruments Inc., Burlingame, CA). Current responses were digitized by A/D converter and analyzed using pClamp 8 (Axon Instruments Inc.) or Origin (Originlab Corp., Northampton, MA), run on an IBM PC. Current-voltage curves were generated by 2-second voltage ramps between −120 and +20 mV. Oocyte capacitance was measured by a paired-ramp method described earlier (Oz et al., 2004a). Briefly, voltage ramps were employed to elicit constant capacitive current (I_{cap}), and the charge associated with this current was calculated by the integration of I_{cap}. Ramps had slopes of 2 V/s and durations of 20 milliseconds and started at a holding potential of −90 mV. A series of 10 paired ramps was delivered at 1-second intervals and averaged traces were used for charge calculations. In each oocyte, the averages of 5–6 measurements were used to obtain values for membrane capacitance (C_m). Currents for I_{cap} recordings were filtered at 20 kHz and sampled at 50 kHz. Current density was calculated by normalizing the average of three consecutive control currents to the oocyte capacitance.

Compounds were applied by addition to the superfusate. All chemicals used in preparing the solutions were from Sigma-Aldrich. 1,2-Bis(*o*-aminophenoxy)ethane-*N,N,N′,N′*-tetraacetic acid (BAPTA), 5-HT, and tropanyl 3,5-dichlorobenzoate (MDL72222) were purchased from Tocris-Cookson (St. Louis, MO). Procedures for the injections of BAPTA (50 nl, 100 mM) were performed as described previously (Oz et al., 1998). Injections were performed 10 minutes prior to recordings using oil-driven ultra microsyringe pumps (Micro4; WPI, Inc., Sarasota, FL). Stock solutions of menthol were prepared in ethanol. Vehicle (ethanol) alone did not affect 5-HT$_3$ receptor function when added at concentrations as high as 0.3% (v/v), a concentration twice as great as the most concentrated application of the agents used. Electrophysiological recordings from oocytes were conducted 2 days after cRNA injections.

Synthesis of cRNA. The cDNA clones of the human 5-HT$_{3A}$ and 5-HT$_{3B}$ subunits were provided by OriGen Inc. (Rockville, MD). cRNAs were synthesized in vitro using a mMessage mMachine RNA transcription kit (Ambion Inc., Austin, TX). The quality and sizes of synthesized cRNAs were confirmed by denatured RNA agarose gels.

Radioligand Binding Studies. Oocytes were injected with 10 ng of human 5-HT$_3$ cRNA, and functional expression of the receptors was assessed by electrophysiology on day 3. Isolation of oocyte membranes was carried out by modification of a method described earlier (Oz et al., 2004b). Briefly, oocytes were suspended (20 μl/oocyte) in a homogenization buffer containing 10 mM HEPES, 1 mM EDTA, 0.02% NaN_3, 50 μg/ml bacitracin, and 0.1 mM phenylmethylsulfonyl fluoride (PMSF) (pH 7.4) at 4°C on ice and homogenized using a motorized Teflon homogenizer (six strokes, 15 seconds each at high speed). The homogenate was centrifuged for 10 minutes at 800*g*. The supernatant was collected and the pellet was resuspended in homogenization buffer and recentrifuged at 800*g* for 10 minutes. Supernatants were then combined and centrifuged for 1 hour at 36,000*g*. The membrane pellet was resuspended in homogenization buffer at the final protein concentration of 0.5–0.7 mg/ml and used for the binding studies.

Binding assays were performed in 500 μl of 10 mM HEPES (pH 7.4) containing 50 μl of oocyte preparation and 1 nM [^{3}H]3-(5-methyl-1*H*-imidazol-4-yl)-1-(1-methylindol-3-yl)propan-1-one ([^{3}H]GR65630) (58.7 Ci/mmol; PerkinElmer Life and Analytical Sciences, Inc., Waltham, MA). Nonspecific binding was determined using 100 μM MDL72222. Oocyte membranes were incubated with [^{3}H]GR65630 in the absence and presence of menthol at 4°C for 1 hour before bound radioligand was separated by rapid filtration onto GF/B filters presoaked in 0.3% polyethylenimine. Filters were then washed with two 5-ml washes of ice-cold HEPES buffer and left in 3 ml of scintillation fluid for at least 4 hours before scintillation counting was conducted to determine amounts of membrane-bound radioligand.

[^{35}S]GTPγS Binding. Oocyte membranes for [^{35}S]GTPγS binding experiments were prepared as described earlier (Lipinsky and Oron, 1996). One hundred fifty oocytes were gently homogenized at 4°C by passing through a 27-gauge needle in 4 ml of homogenization medium [5 mM NaCl, 5 mM Na-HEPES, 0.6 mM PMSF, 4 pM leupeptin (pH 7.5)]. The homogenate was centrifuged for 5 seconds in a conical centrifuge tube at 8000*g*. The supernatant was decanted from the precipitated cellular organelles and the procedure repeated. Following the aspiration of the lipid layer at the surface of the supernatant, it was centrifuged for 20 minutes at 8000*g*. The particulate pellet was resuspended by rehomogenization in 1.8 ml of binding medium [80 mM KC1, 20 mM Na-HEPES, 1 mM MgC1, 1.7 mM PMSF, 0.013 mM leupeptin (pH 7.5)]. Each vial contained (in 25-μl volume) membrane preparation equivalent to one oocyte and the following additions: 45 mM KCl. 11 mM Na-HEPES, 0.5 mM MgCl, 1.0 mM PMSF, 7.3 pM leupeptin (pH 7.5), and 0.5 nM–10 pM [^{35}S]GTPγS. [^{35}S]GTPγS (1000–1500 Ci/mmol) was from New England Nuclear (Boston, MA). Nonspecific binding was assayed by adding 0.5 mM nonradioactive GTPγS and 50 μM ATP. The mixture was incubated at room temperature (22°C) for 30 minutes and filtered rapidly through Whatman (Clifton, NJ) GFIC 25-mm filters and washed with 5 ml of ice-cold wash solution [80 mM KC1, 20 mM Na-HEPES, 1 mM MgC1 (pH 7.5)]. The filters, once washed, were subjected to scintillation counting.

Whole-Cell Patch-Clamp Recording. Nodose ganglion neurons were acutely isolated from adult male Sprague-Dawley rats (200–300 g) as described earlier (Yang et al., 2010a). Briefly, nodose ganglia were rapidly dissected, minced, and dissociated by incubation in type III trypsin (0.75 mg/ml; Sigma-Aldrich), type IA collagenase (1.25 mg/ml; Sigma-Aldrich), and DNase IV (0.125 mg/ml; Sigma-Aldrich) in Dulbecco's modified Eagle's medium (pH 7.4) at 35°C for 25 minutes. Type I-S soybean trypsin inhibitor (1.25 mg/ml; Sigma-Aldrich) was added to stop enzymatic digestion.

The whole-cell patch-clamp technique was was with an Axopatch-1C amplifier and pCLAMP8 software (Axon Instruments Inc.). Neurons were held at −60-mV holding potential and superfused at room temperature (22–24°C) with extracellular solution containing 150 mM NaCl, 5 mM KCl, 2.5 mM $CaC1_2$, 1 mM $MgCl_2$, 10 mM HEPES, 10 mM glucose. Patch electrodes (2–5 MΩ) were filled with an internal solution

containing 140 mM KCl, 2 mM $MgCl_2$, 1 mM $CaCl_2$, 11 mM EGTA, 10 mM HEPES, 2 mM ATP (pH 7.4). Serotonin-containing solutions (with or without drug) were delivered by gravity flow from a linear barrel array consisting of fused silica tubes (i.d. = 200 μm) connected to independent reservoirs; rapid solution exchanges (<50 milliseconds) were achieved by shifting the pipette horizontally using a micromanipulator. The neuron under study was placed within 50 μm of the opening of these tubes and exposed to the desired solution. Culture dishes containing neurons were continuously perfused at 1–2 ml/min with normal external solution. Menthol was diluted in external solution and applied through a gravity-driven perfusion system.

Obtaining a Structural Model of 5-HTR3A. We used the iterative threading assembly refinement (I-TASSER) server (Zhang, 2008) to generate a structural model for 5-HTR3A. To use the server, protocols outlined by Roy et al. (2010) were closely followed. Chain A of the nicotinic acetylcholine receptor (nAChR), under PDB code 2BG9 (Miyazawa et al., 2003), was chosen as the modeling template for a Cys-loop receptor (Thompson et al., 2010). A confidence score (C-Score) was associated by I-TASSER (Roy et al., 2010). The top-scoring model (with C-Score of −2.08) was chosen as a good model for chain A. The top-scoring structure for chain A was aligned with TM-Align (Zhang and Skolnick, 2005) with each of the separate nAChR chains to obtain the same pentameric symmetry in nAChR. The result was a modeled structure for each of the chains, or the complete pentameric structure in 5-HTR3A. Only the transmembrane domain of the modeled structure was employed for docking, as described below.

Docking of L-Menthol on the 5-HTR3A Structural Model. AutoDock 4.2 (Morris et al., 2009) was used to perform rigid docking simulations along with Molecular Graphics Laboratory Tools (MGLTools) Vr. 1.5.4 rev. 30 (Sanner, 1999; Sanner et al., 2002; Morris et al., 2009). Both ligand and receptor files were prepared using recommended procedures described in the MGLTools software documentation (http://mgltools.scripps.edu/documentation). Two torsion angles were specified as parameters for the ligand, while the receptor was modeled as a rigid structure. A grid box area was specified for AutoDock to bind the ligand on relevant regions of the receptor's molecular surface. Choice of the specified grid box area took into account similar binding characteristics believed to be shared by propofol and menthol (Hall et al., 2011) and the close homology of the γ-aminobutyric acid α receptor ($GABA_AR$) to 5-HTR3A (Thompson et al., 2010). Accordingly, the grid box was set to include key residue positions evaluated by Williams and Akabas (2002) for testing propofol binding to the $GABA_AR$-α_1 segment. These positions were mapped onto the 5-HTR3A sequence through a multiple sequence alignment using ClustalW 2.1 (Larkin et al., 2007). Once the grid box area was set to include these residues, docking simulations were performed in AutoDock using the Lamarckian Genetic Algorithm under default parameters. To obtain convergence, the "maximum number of evaluations" was increased to "long." MGLTools was used for analysis of the generated docked configurations for the ligand.

Data Analysis. For the nonlinear curve fitting and regression fits of the radioligand binding data, the computer software Origin was used. In functional assays, average values were calculated as mean ± S.E.M. Statistical significance was analyzed using analysis of variance (ANOVA) or Student's t test, and post hoc Bonferroni test was used following ANOVA. Concentration-response curves were obtained by fitting the data to the logistic equation,

$$y = \{(E_{max} - E_{min})/(1 + [x/EC_{50}]^n)\} + E_{min}$$

where x and y are concentration and response, respectively; E_{max} is the maximal response; E_{min} is the minimal response; EC_{50} is the half-maximal concentration; and n is the slope factor.

Results

Bath application of the specific 5-HT_3 receptor agonist 2-methyl-5-HT (10 μM) caused activation of fast inward currents only in oocytes injected with cRNA transcribed from cloned cDNA encoding human 5-HT_3 receptors (data not shown; n = 12). Currents activated by 1 μM 5-HT were completely inhibited by 0.1 μM LY278584 [1-methyl-*N*-(8-methyl-8-azabicyclo[3.2.1]-oct-3-yl)-1*H*-indazole-3-carboxamide], a specific antagonist of the 5-HT_3 receptor, further indicating that the 5-HT-induced current responses were mediated by the 5-HT_3 receptor–ion channel complex (n = 7).

In our initial studies, (−)-menthol, the most widely occurring isomer in natural sources (Eccles, 1994), was tested. Continuous bath application of (−)-menthol (300 μM) for 15 minutes did not affect membrane resistance (R_m), membrane capacitance (C_m), or resting membrane potential (V_m) in oocytes expressing human 5-HT_3 receptor. A summary of results is presented in Table 1.

Figure 1A presents recordings of 5-HT (1 μM)-induced currents in control conditions (on the left), after 15-minute application of (−)-menthol (100 μM) (in the middle), and after a 20-minute washout period (on the right). Time course of the effects of (−)-menthol application on the maximal amplitudes of 5-HT-induced currents from 5 to 7 oocytes are presented in Fig. 1B. In the presence of vehicle [0.3% (v/v) ethanol], the maximal amplitudes of 5-HT-induced currents remained unaltered during the experiments lasting 45–60 minutes (controls). However, in the presence of 100 μM (−)-menthol, the maximal current amplitudes decreased gradually, reaching steady-state levels within 10–15 minutes. Recovery from menthol effect was slow and usually incomplete during the 15-minute washout period (Fig. 1B).

In the next series of experiments, we examined the concentration-response relationship of the menthol effect on 5-HT_3 receptors (Fig. 1C). The threshold concentration for inhibition by menthol was 30 μM and maximal inhibition was achieved in concentrations ranging between 1 and 3 mM. The inhibition of 5-HT (1 μM)-induced current by 15-minute menthol application was concentration-dependent, with an IC_{50} of 163 ± 14 μM and a slope value of 1.2 (Fig. 1C). Some of the biologic actions of menthol have been shown to be stereospecific (Eccles, 1994). For this reason, we compared the effects of 100 μM of (−), (+), and racemic (±) menthol on human 5-HT_3 receptor. Results indicated that they all similarly inhibited the 5-HT_3 receptors and there were no statistically significant differences in the inhibition caused by these compounds (Fig. 1D; ANOVA, n = 6–8, $P > 0.05$). In the remaining experiments, unless stated otherwise, racemic (±) menthol was used.

In earlier studies, participation of G-protein-coupled receptors (Galeotti et al., 2002) and direct involvement of G-proteins (Klasen et al., 2012; Zhang et al., 2012) in menthol-induced cellular and behavioral responses have been reported. Thus, we tested the effect of menthol in control (distilled water–injected) and pertussis toxin (PTX)-injected oocytes expressing 5-HT_3 receptors. There was no significant

TABLE 1
The effects of menthol (1 mM) on the passive membrane properties of the *X. laevis* oocytes expressing 5-HT_3 receptors

Group	R_m	C_m	V_m
	MΩ	*nF*	*mV*
Control (n = 14)	1.6 ± 0.3	223 ± 27	−42.7 ± 3.6
20-min menthol (n = 16)	1.8 ± 0.4	218 ± 15	−39.8 ± 4.1

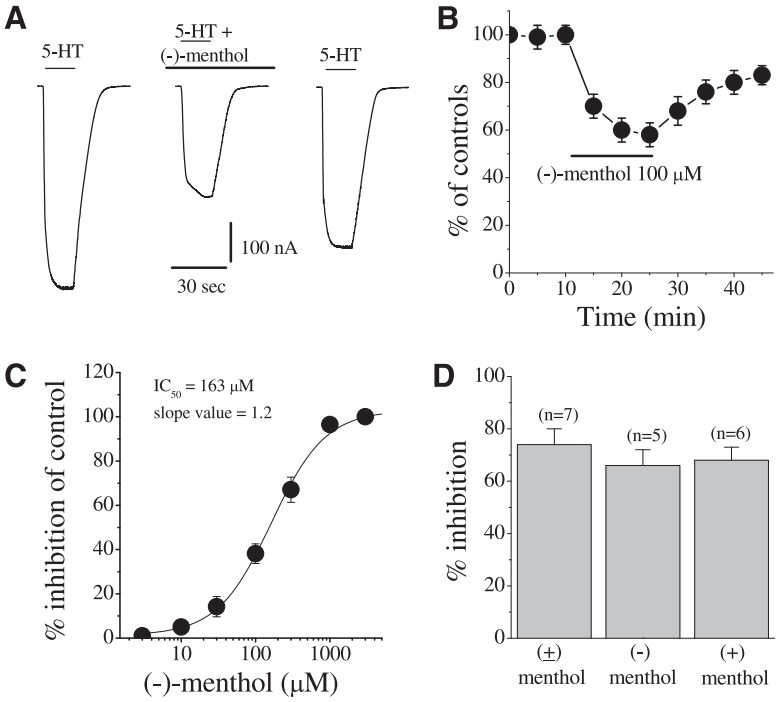

Fig. 1. The effect of menthol on 5-HT$_3$ receptor–mediated ion currents. (A) Records of currents activated by 1 μM 5-HT in control (left), coapplication of 100 μM (−)-menthol and 5-HT after 15-minute (−)-menthol application (middle), and 20-minute washout (right). (B) Time course of the effect of menthol on the currents induced by 1 μM 5-HT at 5-minute intervals. The maximal amplitudes of currents were normalized to first agonist application (at time 0) for each experiment. Solid bar represents application time for vehicle (ethanol, 0.3%) and menthol (100 μM). Data points represent means ± S.E.M. of 7–8 cells. (C) Concentration-response curve for menthol inhibition of 5-HT$_3$ receptor–mediated ion currents. For all concentrations used, menthol was applied for 15 minutes. Data points are the mean ± S.E.M. (n = 5–7); error bars not visible are smaller than the size of the symbols. The curve is the best fit of the data to the logistic equation described in *Materials and Methods*. (D) Comparison of the extent of inhibition caused by 300 μM (+), (−), and racemic forms of menthol application for 15 minutes. Bars represent the means ± S.E.M. from 5 to 7 cells.

difference in menthol inhibition of 5-HT responses between controls and PTX-injected cells (Fig. 2A; ANOVA, n = 5–7, $P >$ 0.05 for the significance of menthol inhibition between controls and PTX group). We also conducted experiments to investigate the effect of menthol (300 μM) on the specific binding of [^{35}S]GTPγS in oocyte membranes. Equilibrium curves for the binding of [^{35}S]GTPγS in the presence and absence of menthol are presented in Fig. 2B (n = 8–9). Menthol did not significantly change the specific binding of [^{35}S]GTPγS. Maximum binding activities (B_{max}) of [^{35}S]GTPγS were 6.4 ± 0.4 and 6.9 ± 0.6 pmol/oocyte (means ± S.E.M.) for controls and menthol, respectively. The apparent affinity (K_D) of the receptor for [^{35}S]GTPγS was 0.91 ± 0.2 and 1.0 ± 0.2 μM for controls and menthol, respectively. There was no statistically significant difference between control and menthol-treated groups with respect to both K_D (ANOVA, n = 8–9, $P > 0.05$) and the B_{max} values (ANOVA, n = 8–9, $P > 0.05$).

In the concentration range used in this investigation, menthol has been shown to increase intracellular Ca^{2+} levels in a wide range of cells in a TRPM8 receptor–independent manner, including skeletal muscle sarcoplasmic reticulum (EC_{50} = 938 μM–1 mM) (Palade, 1987; Neumann and Copello, 2011), tracheal epithelial cells (100 μM–1 mM) (Takeuchi et al., 1994), human leukemia cells (25–100 μM) (Lu et al., 2006), and dorsal horn neurons (100 μM–1 mM) (Tsuzuki et al., 2004). Therefore, we investigated the effect of the Ca^{2+} chelator BAPTA on menthol inhibition of 5-HT responses. In oocytes injected with BAPTA, the inhibition of 5-HT responses by 15-minute menthol (300 μM) application was not significantly different from controls (Fig. 2C; ANOVA, n = 5–6, $P > 0.05$ for the significance of menthol effect between distilled water–injected and BAPTA- injected group).

The mechanisms of menthol actions were further investigated using different application modes of 5-HT and menthol. If menthol acts as an open-channel blocker, it must be present during the channel opening to access its binding site(s). In other words, the extent of menthol inhibition would be independent of its preincubation time. However, the extent of inhibition by menthol was significantly enhanced with prolongation of its preincubation time (Fig. 3A). During these experiments, coapplication of 5-HT and menthol without menthol preincubation was considered as zero point and the menthol inhibition was plotted as a function of preincubation time. Close examination of the time course of menthol actions indicated that the inhibition occurs at fast and slow phases with the respective time constants of $\tau_{1/2fast}$ = 4.2 seconds and $\tau_{1/2slow}$ = 3.4 minutes. Presentation of menthol during constant 5-HT application also induced a rapidly developing inhibition that is consistent with the fast component of menthol inhibition (Fig. 3B). The time course of the recovery from menthol inhibition was considerably slower, within the solution exchange time of the recording system. Interestingly, menthol (300 μM) preincubation alone, without its coapplication with 5-HT, also caused a significant inhibition of the 5-HT-induced currents (Fig. 3C). Menthol preincubation alone did not cause a significant change in desensitization, measured from the linearly decaying portion of 5-HT-induced currents presented in Fig. 3C. Half desensitization time (τ_d) was 10.2 ± 1.4 seconds and 9.7 ± 0.8 seconds in the absence and presence of menthol (paired t test, n = 5, $P < 0.05$).

Without menthol preincubation, coapplication of 5-HT (1 μM) and menthol (300 μM) also inhibited the maximal amplitudes of currents. In the presence of menthol, there was a significant increase in desensitization of 5-HT-induced current (Fig. 3D). A small tail current was also noticeable after the cessation of menthol + 5-HT coapplication.

Recent electrophysiological studies reported that menthol inhibits the functions of Na^+ (Gaudioso et al., 2012; Pan et al., 2012) and Ca^{2+} channels (Pan et al., 2012) in a voltage-dependent manner. The effect of changing the membrane potential relationship between 5-HT-activated current and membrane potential before and after 10-minute menthol (300 μM) application is

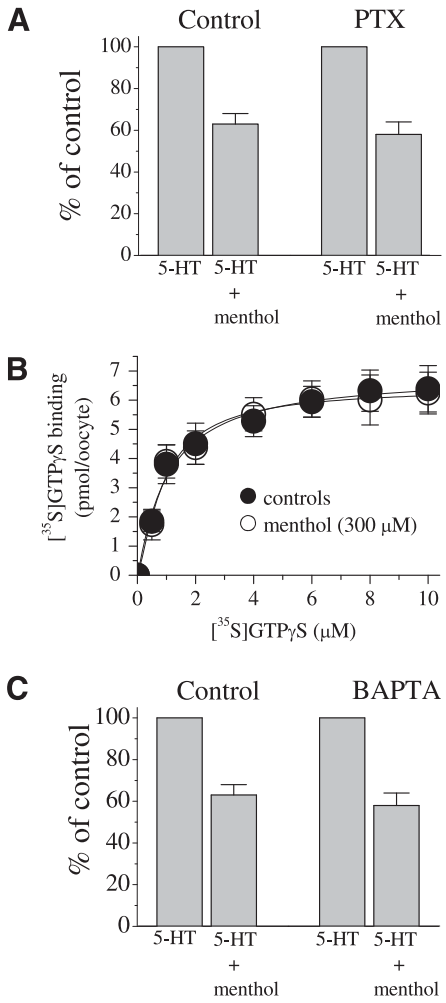

Fig. 2. Effects of menthol on 5-HT_3 receptor–mediated currents in PTX-injected oocytes and on [^{35}S]GTPγS binding of oocyte membranes. (A) The effect of 100 μM menthol application (15 minutes) on the maximal amplitudes of 5-HT-induced currents in oocytes injected with 50 nl distilled water, controls (n = 6), or 50 nl PTX (50 μg/ml; n = 7). Bars represent the means ± S.E.M. (B) The effect of 300 μM menthol on [^{35}S]GTPγS binding to oocyte membrane preparation. Membranes were incubated with different concentrations of [^{35}S]GTPγS for 30 minutes at room temperature, and the results analyzed as described in *Methods*. Data points for controls and menthol are indicated by filled and open circles, respectively (n = 7–8). (C) Bar presentation of the effects of 1 μM menthol application (20 minutes) on the maximal amplitudes of 5-HT-induced currents in oocytes injected with 50 nl distilled water [controls (n = 5)] or 50 nl of BAPTA (200 mM; n = 7). Bars represent the means ± S.E.M.

shown in Fig. 4A. Examination of the voltage dependence of the menthol actions indicated that the degree of the inhibition of the 5-HT (1 μM)-induced currents tended to increase with depolarizing membrane potentials (Fig. 4B). Compared with −120 mV, the difference in the extent of menthol inhibition reached statistically significant levels at 0 and +20 mV (paired t test, n = 6–7, $P < 0.05$). The small tail current observed after the cessation of menthol + 5-HT coapplication (Fig. 3D), together with a relatively weak voltage dependence of menthol inhibition, is in agreement with open-channel blockade. However, because of possible variations in solution-exchange time and drug application speeds among different oocyte recordings and difficulties inherent to the oocyte expression system, we were not able to record and analyze these tail currents consistently.

Considering the time courses of menthol actions (Fig. 3A), we hypothesized that two binding sites with fast and slow kinetics may differentially contribute to voltage dependency of menthol inhibition. For this purpose, we have compared the extent of voltage-dependent inhibition at two time points, without preincubation (during coapplication of 5-HT + menthol) and after 10-minute menthol preincubation. Without preincubation, the extent of menthol inhibition at depolarized membrane potentials was significantly elevated. For example, compared with −120 mV, menthol inhibition at +20 mV was 18 ± 2% higher (n = 4–5). However, following 10-minute preincubation, this difference was reduced significantly to 3 ± 1% (paired t test, n = 4–5, $P < 0.05$).

Menthol may alter 5-HT_3 receptor function via competitive inhibition of 5-HT binding to the receptor. To examine this possibility, the concentration-response curve of 5-HT was examined in the absence and presence of 300 μM menthol. The EC_{50} values in the absence and presence of menthol were 1.2 ± 0.2 and 3.2 ± 0.3 μM (means ± S.E.M.), respectively (n = 5–7). As shown in Fig. 5A, menthol did not significantly alter EC_{50} values and inhibited the maximal 5-HT responses to the same percentage of control values, suggesting that menthol is a noncompetitive inhibitor of 5-HT_3 receptors. In radioligand binding experiments, 5-HT concentration-dependently inhibited the specific binding of 1 nM [^{3}H]GR65630 (Fig. 5B). The concentration-dependent inhibition of [^{3}H]GR65630 binding by 5-HT was not altered by 300 μM menthol (Fig. 5B). The IC_{50} values in the absence and presence of menthol were 561 ± 169 and 639 ± 177 nM, respectively (ANOVA, n = 8–11, $P > 0.05$). Similarly, increasing menthol concentrations did not reduce specific [^{3}H]GR65630 binding to membranes of oocytes expressing 5-HT_3 receptor cDNA (Fig. 5C).

Menthol does not appear to alter agonist displacement of 5-HT_3 antagonist binding, suggesting no change in agonist affinity. Interpretation of radioligand studies is complicated by the fact that radioligand binding is performed under conditions in which receptors are predominantly in the desensitized/high-affinity state (for a discussion, see Lovinger and Zhou, 1993). However, agonist binding is not independent of channel state since open and desensitized receptors are necessarily agonist-bound, and thus any effect that stabilizes these states may alter apparent agonist affinity. Electrophysiological studies in various types of mammalian cells (Lovinger and Zhou, 1993) and an oocyte expression system (Oz et al., 2003) indicate that in contrast to 5-HT, dopamine (DA) gates 5-HT_3 receptors with low efficacy because peak currents evoked by receptor-saturating concentrations of DA are significantly smaller than those evoked by 5-HT. Therefore, in this study, we used the inefficacious 5-HT_3 agonist DA (1 mM) to resolve the effects of menthol on 5-HT_3 receptor agonist binding affinity and channel gating efficacy. We compared the effect of menthol between 5-HT and DA responses. The inhibition of DA-induced currents by 15-minute menthol (300 μM) application was not significantly different from controls (Fig. 5D; ANOVA, n = 5–6, $P <$ 0.05 for the significance of menthol effect between DA and 5-HT-activated currents).

Monoterpenes such as menthol and thymol display close structural similarities to propofol (Watt et al., 2008). Furthermore, menthol and propofol share general anesthetic activity and common interaction sites for activation of $GABA_A$Rs (Watt et al., 2008; Zhang et al., 2008). In fact, recent studies indicated

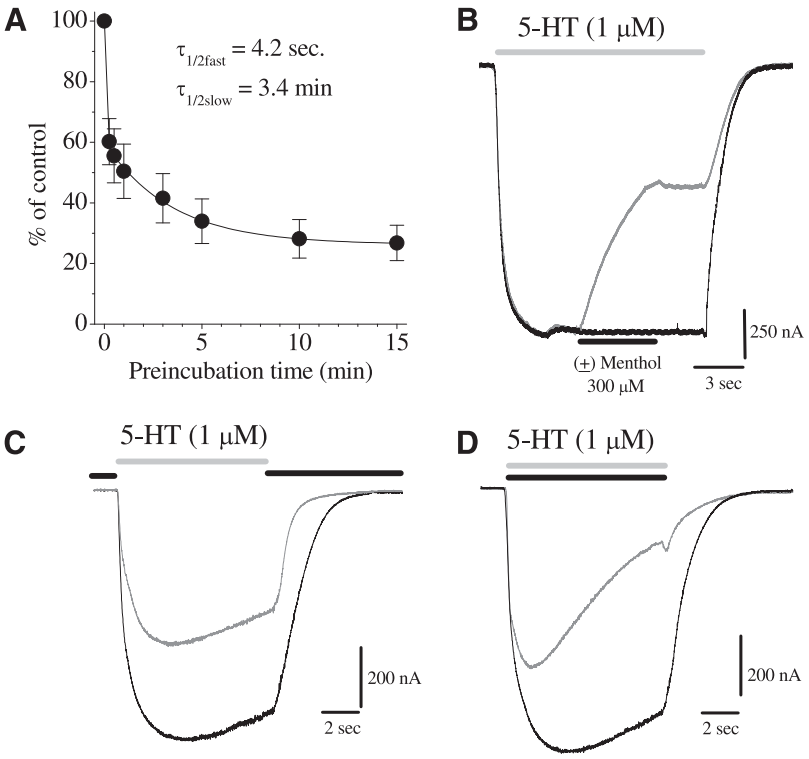

Fig. 3. The effect of increasing menthol preincubation time and different menthol application modes on the 5-HT$_3$ receptor–mediated currents. (A) Time course of menthol inhibition as a function of menthol preincubation time. The solid curve shows a best fit for the data points; an exponential decay with two time constants, τ_{fast} and τ_{slow}, is shown in the figure. Each data point represents the means ± S.E.M. from 7 to 8 oocytes. (B) The effect of introducing 300 μM menthol after activation of currents by 5-HT (1 μM). The solid gray bar on the top of the current trace represents the 5-HT application time. The duration of menthol application, indicated with solid black bar, is presented below current trace. The small transient current fluctuation before the menthol application is due to change between two 5-HT application tubes to test the contribution of a possible mechanical artifact during solution exchange in the chamber. Calibration bars are indicated in the panel. (C) The effect of menthol application before and after 5-HT application. Menthol (300 μM) application time is indicated with solid gray bars. Menthol was present in the bath only before and after, but not during, 5-HT application. (D) The effect of menthol and 5-HT coapplication, without menthol preincubation, on the 5-HT$_3$ receptor–mediated currents. Menthol was applied only in the presence of 5-HT.

that the mutations causing decreased propofol actions on GABA$_A$Rs also affect menthol potentiation of these receptors (Watt et al., 2008). In an attempt to identify chemical moieties that modulate the inhibitory effect of menthol, we divided the compounds into two subgroups, namely the unsubstituted congeners cyclohexane and eucalyptol and the OH-substituted derivatives menthol and propofol. Within the unsubstituted derivatives, cyclohexane was the least active one, showing an inhibition potency of <5% at 100 μM application. Likewise, the ether derivative eucalyptol, with increased lipophilic character, appeared to exhibit a detectable increase in its potency when compared with cyclohexane, suggesting that the presence of hydrogen-accepting oxygen might contribute in modulating the inhibitory affinity of eucalyptol with the 5HT$_{3A}$ receptor protein (Fig. 6A). In contrast, introduction of an aliphatic hydroxyl group as present in menthol or even an aromatic one in propofol potently enhanced their inhibitory effect on 5-HT$_{3A}$ receptor, thus significantly increasing the inhibition observed for menthol as well as propofol in the current study (Fig. 6A). Inhibition by these compounds increased in the order of cyclohexane > eucalyptol > menthol > propofol (Fig. 6A).

We next investigated whether cyclohexane, eucalyptol, menthol, and propofol interact functionally on the 5-HT$_3$ receptor (Fig. 6B). In this set of experiments, the effects of the compounds were tested within the same cell to minimize the variations between cells. Bath application of 100 μM cyclohexane alone (for 15 minutes) did not affect the maximal amplitudes of 5-HT-induced current. However, the inhibitory effect of menthol was enhanced significantly in the copresence of cyclohexane and menthol (Fig. 6B; ANOVA, $n = 6$, $P < 0.05$). In agreement with earlier findings (Rusch et al., 2007), propofol inhibited 5-HT$_3$ receptors. However, there was no statistically significant difference between the extent of inhibition caused by coapplication of menthol and propofol or the sum of the inhibitory actions of menthol alone and propofol alone (Fig. 6B). Similarly, only additive action (neither occlusive nor synergistic actions) was observed for menthol and eucalyptol coapplications (Fig. 6B), suggesting that other than cyclohexanol, there is no functional interaction among the binding sites of propofol, eucalyptol, and menthol.

Subunit composition of 5-HT$_3$ receptors has been shown to influence modulation of the receptor function by various drugs (Thompson and Lummis, 2007; Barnes et al., 2009). Therefore, we tested whether the coexpression of A and B subtypes would alter the extent of menthol inhibition. Results indicated that the difference in the extent of menthol inhibition was not statistically significant between 5-HT$_{3A}$ and 5-HT$_{3AB}$ receptor subtypes (Fig. 7A; ANOVA, $n = 5–7$, $P > 0.05$).

In the next set of experiments, we investigated whether menthol acts on 5-HT$_3$ receptors expressed natively in neuronal structures. For this purpose, we tested the effect of 100 μM menthol on 5-HT$_3$ receptor–mediated currents recorded in acutely dissociated adult rat nodose ganglion neurons. Figure 7 illustrates a decrease in the amplitude of 5-HT (10 μM)-induced currents by 15-minute bath application of 100 μM menthol. In seven neurons tested, the average inhibition by 100 μM menthol application was 61 ± 7% (Fig. 7B). Menthol in 100 μM and higher concentrations caused a slowly developing (within a minute) inward current in ~40% (5/12) of the nodose ganglion neurons tested, and these neurons were not included in the present study. Responses to menthol applications have been described in earlier studies in these neurons and suggested to be due to activations of TRPM8 and TRPA1 receptors (Fajardo et al., 2008).

A bioinformatics procedure to evaluate L-menthol (1*R*,2*S*,5*R*) binding to the 5-HT$_3$ receptor was used. A structure for the L-menthol ligand (ZINC ID: 01482164) was obtained from the

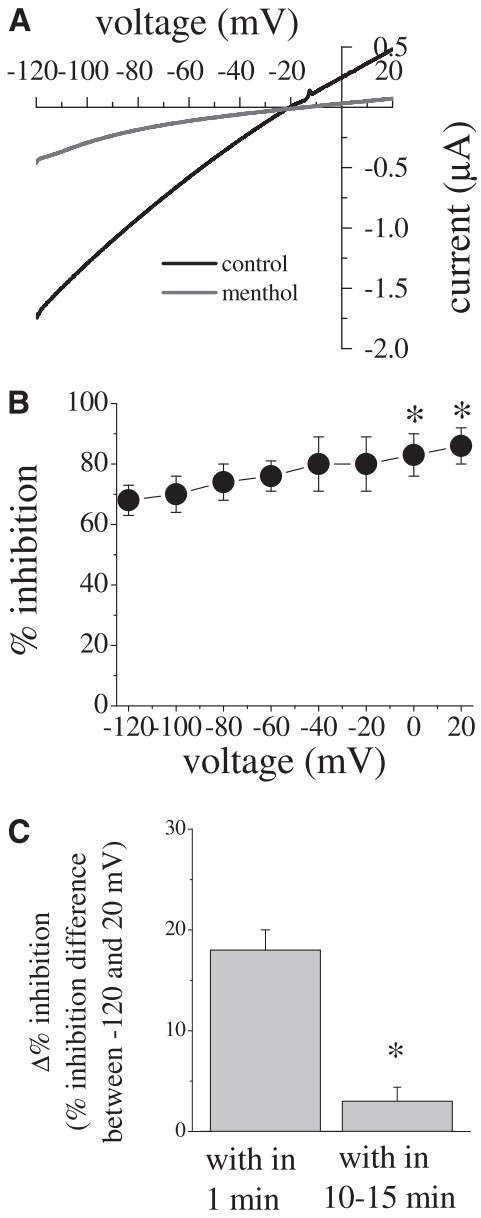

Fig. 4. The effect of membrane potential changes on menthol inhibition of 5-HT_3 receptor–mediated ion currents. (A) Current-voltage relationship of 5-HT-activated current in the absence (black trace) and presence (gray trace) of 300 μM menthol. Currents were activated by 1 μM 5-HT in the same oocyte. (B) Percentage inhibition of 5-HT-activated current by 300 μM menthol at different membrane potentials; there are no significant differences among these values at different membrane potentials (ANOVA, $n = 5$, $P > 0.05$). (C) Time-dependent alterations in the voltage dependency of menthol inhibition. Current traces in response to voltage ramps were recorded within 1 minute of coapplication of 5-HT and menthol and compared with those recorded after 10 minutes of menthol application (ANOVA; $n = 6$, $P < 0.05$).

ZINC Vr. 12 Database (Irwin et al., 2012). In choosing the 5-HTR3A sequences, a longer 516-amino-acid human isoform (Uniprot AC: P46098-5) was considered to include several splice variants. A docking method was used to test for L-menthol direct binding to the predicted 5-HT_3 receptor structure. Figure 8A shows key residues for the association of the L-menthol ligand, identified through a multiple sequence alignment of the 5-HT_3 receptor (see *Materials and Methods*). These key residues, which were used to define the area of interest for docking through the grid specification mechanism, are annotated by the red triangle at THR361 in Fig. 8A. Position THR361 appears directly involved in the interaction between menthol and nAChR (used to model the Cys-loop receptor as described in *Materials and Methods*). Since our modeling procedure to obtain a structure for the 5-HT_3 receptor uses the existing α7 nAChR crystal structure as a template, it is to be expected that structural similarity may result in similar binding sites for menthol between the 5-HT_3 receptor and the nAChR. Indeed, our docking simulations for L-menthol on 5-HTRA resulted in a number of low-energy configurations for L-menthol that were stabilized by interactions with THR361. This particular docked configuration of the ligand is shown circled in black, in two different viewing angles in Fig. 8B, panel 1 (top-down view) and panel 2 (side view). Figure 8B (panels 3 and 4) demonstrates that an h-bond between menthol and THR361 (at a distance of 1.81 Å) stabilizes the ligand onto the predicted receptor structure. MGLTools analysis reports a binding energy of −6.35 kcal/mol for this ligand configuration, suggesting that residue THR361 plays a central role in L-menthol binding to 5-HT_3 receptors. A number of docking simulations also resulted in low-energy configurations that placed the ligand in contact with residue ASP266 (data not shown). The two predicted residues, THR361 and ASP266, might thus constitute a naturally occurring binding site for menthol on 5-HT_3 receptors.

Discussion

The results indicate that menthol reversibly inhibits the function of human 5-HT_3 receptors expressed in *X. laevis* oocytes in a concentration-dependent manner, with an IC_{50} value of 163 μM. The results of both electrophysiological and radioligand binding studies indicated that menthol does not compete with the 5-HT binding site on the receptor.

In earlier studies, participation of G-protein-coupled receptors such as κ-opioid receptors (Galeotti et al., 2002) and direct involvement of G-proteins (Klasen et al., 2012; Zhang et al., 2012) in menthol-induced cellular and behavioral responses have been reported. However, the results indicate that activity of G-proteins remained unchanged in the presence of menthol. Menthol has been shown to increase intracellular Ca^{2+} levels and activate various Ca^{2+}-sensitive kinases (Farco and Grundmann, 2013). In an oocyte expression system, alterations in intracellular Ca^{2+} levels can be examined indirectly by monitoring the holding current under voltage-clamp conditions since Ca^{2+}-activated Cl^- channels in oocytes are highly sensitive to Ca^{2+} (for a review, see Dascal, 1987). However, menthol application alone (up to 1 mM at room temperature of 21–23°C) did not induce changes in holding currents, suggesting that menthol did not alter intracellular Ca^{2+} levels in *X. laevis* oocytes. Furthermore, menthol continued to inhibit 5-HT_3 receptors to a similar extent in BAPTA-injected oocytes, further suggesting that changes in intracellular Ca^{2+} levels are not involved in menthol inhibition of 5-HT_3 receptors.

Menthol, as a result of its lipophilic character, preferentially partitions from an aqueous phase into membrane structures (Trombetta et al., 2005; Turina et al., 2006). Partitioning of these lipophilic substances has been suggested to result in increased membrane fluidity, permeability, and disturbance of membrane integrity. However, passive membrane properties such as membrane capacitance, resting membrane potential,

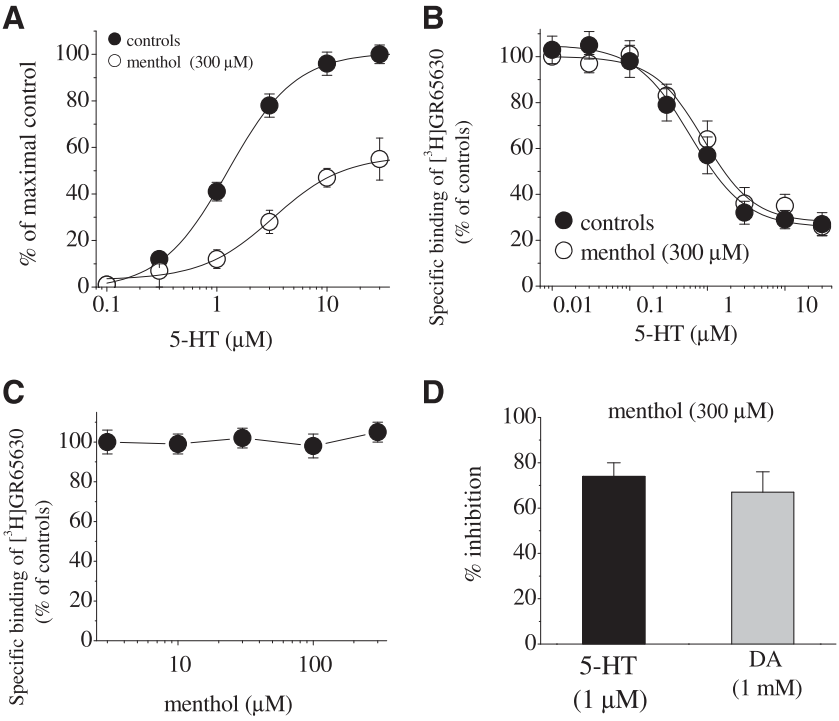

Fig. 5. The effect of menthol on 5-HT concentration-response curves and the specific binding of [^{3}H]GR65630 on *X. laevis* oocytes expressing 5-HT$_3$ receptors. (A) Concentration-response curves for 5-HT-activated current in the absence (filled circles) and presence (open circles) of 300 μM menthol. Currents were activated by 5-HT concentrations ranging from 0.1 to 100 μM. Menthol was applied for 20 minutes, and 5-HT and menthol were then coapplied for 10–15 seconds. Data points are the mean ± S.E.M. (n = 5–6). The curve is the best fit of the data to the logistic equation described in *Materials and Methods*. The control concentration-response curve is normalized to the maximal response. The concentration-response curve in the presence of menthol is the percentage of the maximal control. (B) Inhibition of specific [^{3}H]GR65630 binding by non-labeled 5-HT in membranes after 1-hour preincubation with 300 μM menthol. The concentration of [^{3}H]GR65630 was 1 nM. The inhibition curve shows pooled data from 8 to 11 measurements from three experiments. (C) Effects of increasing concentration of menthol on the specific binding of [^{3}H]GR65630. Experiments were conducted in the presence of 1 nM [^{3}H]GR65630. The results present data from 8 to 11 measurements. Data points indicate mean ± S.E.M. (D) Comparison of the effect of 15-minute application of 300 μM menthol on the maximal amplitudes of currents induced by 5-HT (1 μM) and DA (1 mM). There was no statistically significant difference among the bars (ANOVA, n = 7–8, $P > 0.05$).

and oocyte input resistance were not significantly influenced by menthol (Table 1), suggesting that in the concentrations used in this study, menthol did not disrupt the integrity of the lipid membrane.

Our results provide the first demonstration that menthol directly inhibits the function of human 5-HT$_3$ receptors in clinically relevant concentrations. In a recent study (Heimes et al., 2011), 5-HT-induced [^{14}C]guanidinium influx mediated by natively expressed voltage-sensitive Na^+ channels and 5-HT$_3$ receptors in NIE-115 cells (Barann et al., 1999) was significantly inhibited by menthol (estimated IC_{50} value is in the range of 100–300 μM), further suggesting that menthol can modulate the function of 5-HT$_3$ receptors. Similarly, in rat ileum smooth muscle (Heimes et al., 2011), 5-HT-induced muscle contractures thought to be mediated by 5-HT$_3$ receptors were also suppressed by menthol (with an estimated IC_{50} value of 200–600 μM). In agreement with these findings in rodents, our patch-clamp studies in rat nodose ganglion neurons also indicate that menthol inhibits 5-HT$_3$ receptor–mediated currents. Although actions of several drugs have been reported to be modulated by subunit combinations (for reviews, see Thompson and Lummis, 2007 and Barnes et al., 2009), there was no statistically significant difference in menthol inhibition between 5-HT$_{3A}$ and 5-HT$_{3AB}$ receptors in our study.

In earlier studies, menthol in the concentration ranges used in this study has been shown to act directly on GABA$_A$ (EC_{50} = 1.1 mM) (Pan et al., 2012), glycine (100–300 μM) (Hall et al., 2004), and ryanodine receptors (1 mM) (Palade, 1987; Neumann and Copello, 2011). Both ligand-gated and voltage-gated channels are inhibited by menthol (IC_{50} = 297 μM for Na^+ channels and IC_{50} = 125 μM for Ca^{2+} channels in dorsal horn neurons) (Pan et al., 2012). Moreover, the effective concentrations observed in the current study were found to be comparable with menthol concentrations sufficient to activate TRPM8 channels, with EC_{50} values ranging between 67 and 196 μM (Sherkheli et al., 2010) in *X. laevis* oocytes. However, menthol also nonselectively activates TRPV3 (EC_{50} = 20 mM) and inhibits mouse TRPA1 (IC_{50} = 68 μM) (Macpherson et al., 2006). In our study, the concentration of menthol effective on 5-HT$_3$ receptors ranged from 30 μM to 1 mM (IC_{50} = 163 μM). These concentrations approximate those used in human psychophysical studies and are considerably lower than those used in over-the-counter products (≈500 mM) (Yosipovitch et al., 1996; Namer et al., 2005). Menthol taken orally is effectively absorbed in gastrointestinal mucosa and can easily reach the range of menthol concentrations used in this study. Menthol undergoes extensive enterohepatic recirculation, and it is rapidly but incompletely (~50%) metabolized to menthol glucuronide, which is excreted both in the bile and in the urine (Gelal et al., 1999). In a recent study, a high concentration of menthol (54 μg/g) was detected in brain tissue 5 minutes after 100-mg/kg intraperitoneal injection (Pan et al., 2012), indicating that menthol is rapidly absorbed into the brain. Therefore, functional modulation of 5-HT$_3$ receptors demonstrated in this study can mediate some of the pharmacological actions of menthol.

Menthol is known to act stereoselectively in some, but not all, in vivo and in vitro assay systems (for reviews, see Eccles, 1994 and Farco and Grundmann, 2013). In an earlier study, Hall et al. (2004) showed that the effect of menthol on GABA$_A$ currents were stereoselective, with (+)-menthol being more potent than (−)-menthol, while menthol modulation of glycine receptors did not display stereospecificity. In our study, we could not detect a stereoselectivity of menthol actions on 5-HT$_3$ receptors (Fig. 1).

Allosteric modulators alter the functional properties of ligand-gated ion channels by interacting with site(s) that are topographically distinct from the ligand binding sites (for a review, see Onaran and Costa, 2009). In electrophysiological studies, although the potency of 5-HT, a natural ligand

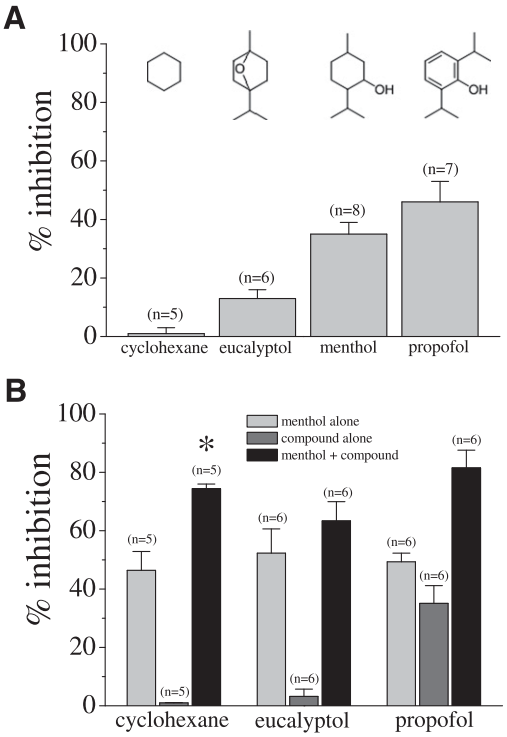

Fig. 6. Comparison of the effects of some compounds structurally related to menthol on the 5-HT_3 receptors. (A) Comparison of the effects of equimolar concentrations (100 μM) of cyclohexane, eucalyptol, propofol, and menthol on 5-HT_3 receptors. Bars represent the means ± S.E.M. (n = 5–8). Chemical structures of the compounds are presented at the top of each bar. (B) Comparison of the interaction between menthol and other structurally similar compounds on the currents activated by 5-HT in the same oocytes. Bars represent the means ± S.E.M. (n = 5–6).

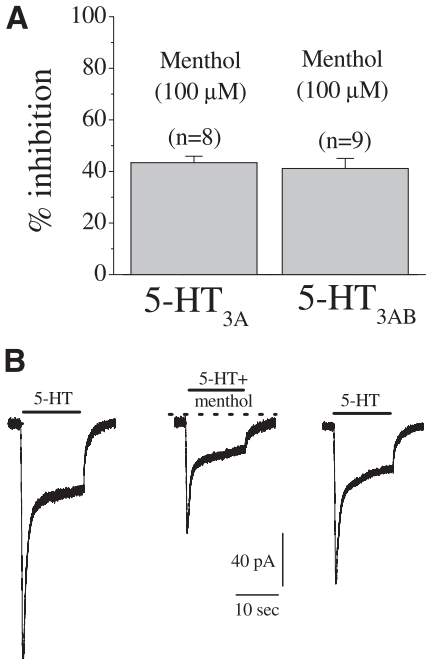

Fig. 7. The effect of menthol on A and AB subunit combination of human 5-HT_3 receptors expressed in *X. laevis* oocytes and 5-HT-induced currents recorded in acutely dissociated nodose ganglion neurons. (A) Comparison of the effect of 100 μM menthol on the human 5-HT_{3A} and 5-HT_{3AB} receptors expressed in oocytes. Bar graph shows average inhibition (mean ± S.E.M.) of 5-HT (1 μM)-induced currents by 15-minute menthol application in 5–7 oocytes. (B) Records are sequential (from left to right) current traces obtained from a single nodose ganglion neuron voltage-clamped at −60 mV. Currents activated by 3 μM 5-HT before (left) and after 10-minute application of 100 μM menthol (middle), and recovery of 5-HT-induced current after 15-minute washout period (right).

(agonist) for this receptor, was not altered, its efficacy was significantly inhibited by menthol, indicating that menthol does not compete with the 5-HT binding site on the receptor. In agreement with these findings, radioligand binding studies indicated that displacement of [^{3}H]GR65630 (competitive antagonist of 5-HT_3 receptors) by 5-HT was not significantly affected by menthol, further suggesting that menthol does not interact with the 5-HT binding site on the human 5-HT_3 receptor. In an earlier report on NG101 cell lines (Heimes et al., 2011), menthol did not affect the radioligand binding site on the 5-HT_3 receptor. Similarly, 5-HT (up to 0.1 mM tested in this study) did not affect specific binding of [^{32}H]menthol to membranes from guinea pig lung (Wright et al., 1998). In an earlier study, binding of [^{32}H]flunitrazepam to $GABA_A$Rs in primary cultures of mouse cortical neurons was not affected by concentrations of up to 1 mM menthol (Garcia et al., 2006). The results of functional studies together with radioligand binding experiments suggest that menthol does not compete with the 5-HT binding site, but it acts as an allosteric inhibitor of the 5-HT_3 receptor.

In recent studies, menthol in the concentration range used in this study has been reported to be an allosteric modulator of $GABA_A$ (Hall et al., 2004) and $\alpha4\beta2$ nicotinic receptors (Hans et al., 2012); i.e., menthol binds to site(s) topographically distinct from the agonist sites on these receptor. Under physiologic conditions, the noncompetitive property of the allosteric menthol inhibition may be advantageous since the increases in concentration of endogenous agonist (5-HT) in the synaptic cleft to millimolar concentrations cannot alter the efficacy of menthol on the receptor. DA competes with the 5-HT binding site, but activates these receptors with lower efficacy and causes considerably less desensitization. Since a saturating concentration of DA was used in the present study, menthol inhibition could not have resulted from fewer channels in a desensitized state or from a decrease in agonist affinity.

Based on the kinetics of menthol's effect (the fast and slow components of inhibition in Fig. 3A), it is likely that multiple allosteric binding sites are involved in the interaction of this molecule with the 5-HT_3 receptor. In agreement with this hypothesis, coapplication of 5-HT and menthol (Fig. 3, A and C), without preincubation, also induces fast inhibition of 5-HT-induced currents by blocking the channel pore or promoting the desensitization of the receptor (Dopico and Lovinger, 2009).

Open-channel blockade is a widely used model to describe the inhibition of functions of various ion channels. Tail currents seen after the cessation of menthol application and, although weak, the voltage sensitivity of its action is in favor of open-channel inhibition. However, an open-channel model cannot account for all of the findings of the present study. First, for open-channel blockers, the presence of the agonist is required to let the blocker enter the channel after the receptor was opened by the agonist. However, preincubation of menthol caused significant further inhibition (Figs. 1A and 3A), indicating that the compound can also interact with the closed state of the 5-HT_3 receptor. Second, the proportion of

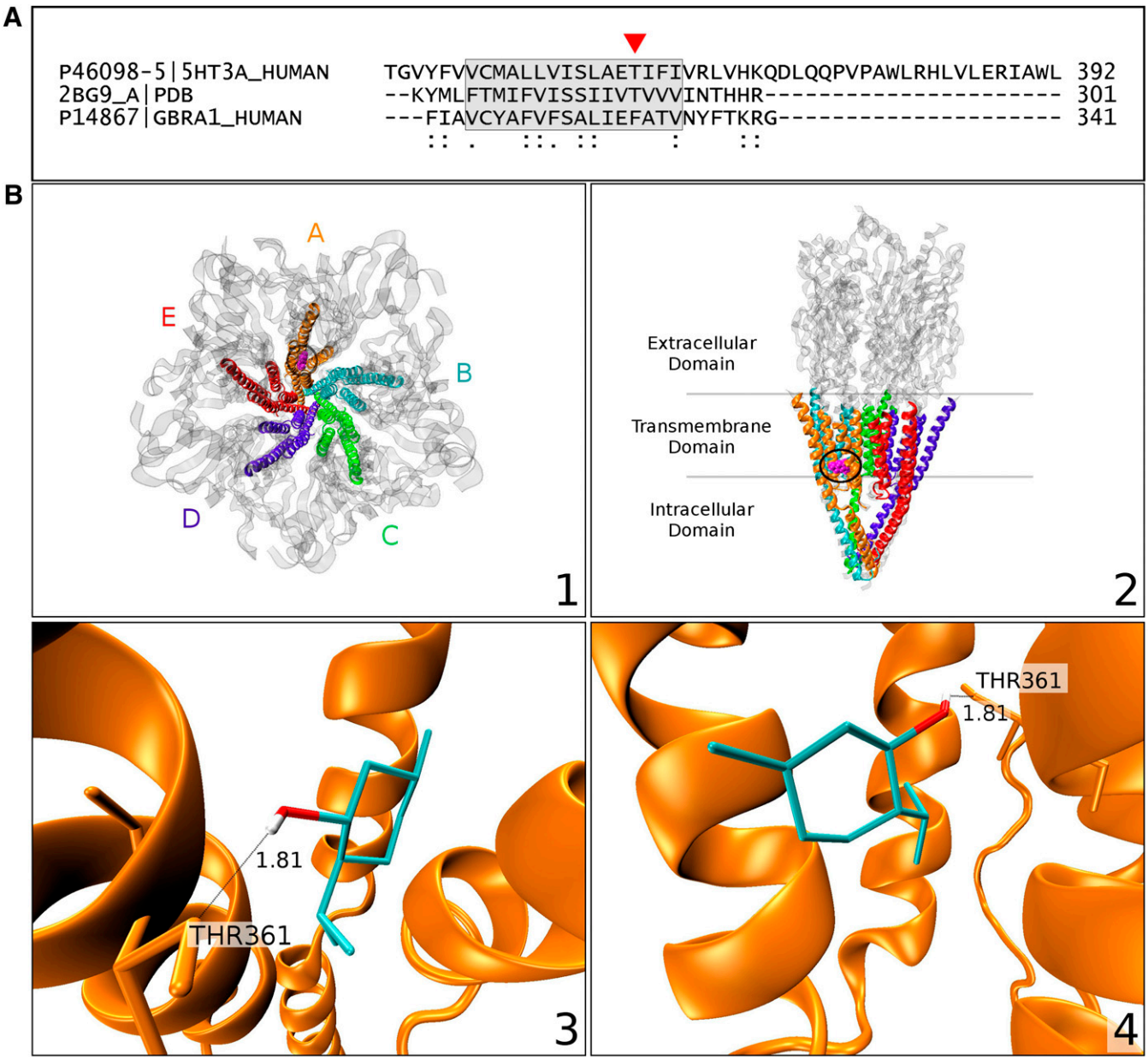

Fig. 8. (A) A multiple sequence alignment obtained with ClustalW 2.1 between the human GABA$_A$R-α_1 subunit (UniProt AC: P14867), the α7 nAChR chain A (Miyazawa et al., 2003; PDB code 2BG9), and the human 5-HT$_3$ receptor (UniProt AC: P46098-5). Boxed and shaded regions indicate key residue positions from the M3 segment of GABA$_A$R-α_1 evaluated by Williams and Akabas (2002) for propofol binding. Docking simulations show L-menthol binding at the position indicated by the red triangle. (B) Panels 1 and 2: A bioinformatics model of the pentameric structure for the 5-HT$_3$ receptor (top-down view in panel 1 and side view in panel 2), with nAChR drawn in translucent gray for reference. All 5-HT$_3$ receptor chains are of the same primary sequence; chain letters refer to the nAChR chains with which the modeled chain for 5-HTR3A was aligned to obtain the pentameric symmetry for 5-HTR3A. Chain A is colored in orange, B in cyan, C in green, D in violet, and E in red. The binding site for the ligand is circled in black. Panels 3 and 4: A representative lowest-energy (−6.35 kcal/mol) configuration for the L-menthol ligand in two different views. The h-bond that stabilizes the ligand onto the 5-HTR3A structure is formed with residue THR361 at a distance of 1.81 Å.

somewhat weak voltage sensitivity of menthol inhibition observed at the early phase of the menthol application diminished significantly after 10-minute menthol incubation.

Menthol, a highly lipophilic agent, first dissolves into the lipid membrane (Turina et al., 2006) and then diffuses into a nonannular lipid space to inhibit the ion channel–receptor complex (Sanghvi et al., 2009). Consistent with this idea, the effect of menthol on 5-HT$_3$ receptors reached a maximal level within 10–15 minutes of application. Similarly, actions of several hydrophobic allosteric modulators (McCool and Lovinger, 1995; Oz et al., 2002a,b) on 5-HT$_3$ receptors require several minutes (5–20 minutes) of application time to reach their maxima (for a review, see Oz, 2006), suggesting that the binding site(s) for these allosteric modulators are located inside the lipid membrane and that drug exposure time rather than channel opening is essential for menthol inhibition of the receptor. Thus, it appears that menthol can interact with 5-HT$_3$ receptors during the closed state. Overall, it is likely that at least two binding sites mediate menthol's actions on 5-HT$_3$ receptors. One of the sites is either causing open-channel

blockade or promoting desensitization of the receptor (Dopico and Lovinger, 2009) and is weakly sensitive to transmembrane electric field. Another binding site located in the bilayer lipid membrane (Trombetta et al., 2005; Turina et al., 2006) has access to the closed state of the channel-receptor complex and diminishes the percent contribution of the voltage-sensitive binding site to the total amount of inhibition.

It is plausible that menthol reduces current amplitude by lowering the energy barrier for receptors to enter a desensitized and/or closed state. This mechanism has already been proposed for nicotinic receptors (Spivak et al., 2007). Clearly, further investigations in which receptor kinetics can be studied in a more detailed and precise manner are required to delineate the mechanisms of menthol actions on 5-HT_3 receptor function.

Evaluation of the data in Fig. 6 provided evidence that combining menthol with either eucalyptol or propofol enhanced its inhibitory effect on 5HT-induced currents, suggesting that these compounds have additive effects on 5-HT_3 receptors (Fig. 6B). On the other hand, cyclohexane (100 μM) alone displayed undetectable efficacy at inhibiting 5-HT_{3A} receptors, but increased significantly the potency of menthol, suggesting that cyclohexane may facilitate the interaction of menthol with its binding site on the receptor (Fig. 6B). Our results also indicate that the extent of $5HT_3$ receptor inhibition varied with the substitution pattern on the cyclohexane skeleton and that an aromatic hydroxyl group as present in propofol has the highest potency in inhibiting 5HT3A receptor. The results observed for the parent compound cyclohexane and derivatives thereof may be useful in further understanding the molecular mechanisms involved in pharmacological effects of menthol as well as propofol.

Menthol is a monoterpenoid, and other monoterpenoids such as borneo, thymol, menthone, camphor, and carvone have been shown to potentiate $GABA_A$ and glycine receptors (Priestley et al., 2003; Hall et al., 2004). In an earlier study, camphor has also been shown to inhibit nicotinic receptor–induced norepinephrine secretion and Ca^{2+} increases in bovine adrenal chromaffin cells (Park et al., 2001).

In conclusion, our results indicate that menthol inhibits the function of homomerically expressed human 5-HT_3 receptor by a noncompetitive mechanism. These data add to a growing body of evidence (Farco and Grundmann, 2013) suggesting that in addition to TRPM8 receptors, other target proteins such as 5-HT_3 receptors can also contribute to the pharmacological actions of menthol.

Acknowledgments

The authors thank Dr. David Lovinger of the Intramural Research Program (IRP) of the National Institute on Alcohol Abuse and Alcoholism IRP for constructive comments and valuable suggestions and Dr. Mary Pfeiffer of the IRP of the National Institute on Drug Abuse for careful editing of the manuscript.

Authorship Contributions

Participated in research design: Shuba, Yang, Shehu, Kabbani, Sadek, Howarth, Oz.

Conducted experiments: Ashoor, Nordman, Veltri, Al Kury.

Contributed new reagents or analytic tools: Shehu, Yang, Veltri.

Performed data analysis: Ashoor, Nordman, Veltri, Al Kury, Kabbani, Shehu, Oz.

Wrote or contributed to the writing of the manuscript: Ashoor, Oz, Kabbani, Shehu.

References

Barann M, Göthert M, Brüss M, and Bönisch H (1999) Inhibition by steroids of [14C]-guanidinium flux through the voltage-gated sodium channel and the cation channel of the 5-HT3 receptor of N1E-115 neuroblastoma cells. *Naunyn Schmiedebergs Arch Pharmacol* **360**:234–241.

Barnes NM, Hales TG, Lummis SC, and Peters JA (2009) The 5-HT3 receptor—the relationship between structure and function. *Neuropharmacology* **56**:273–284.

Cappello G, Spezzaferro M, Grossi L, Manzoli L, and Marzio L (2007) Peppermint oil (Mintoil) in the treatment of irritable bowel syndrome: a prospective double blind placebo-controlled randomized trial. *Dig Liver Dis* **39**:530–536.

Dascal N (1987) The use of *Xenopus* oocytes for the study of ion channels. *CRC Crit Rev Biochem* **22**:317–387.

de Araújo DA, Freitas C, and Cruz JS (2011) Essential oils components as a new path to understand ion channel molecular pharmacology. *Life Sci* **89**:540–544.

Dopico AM and Lovinger DM (2009) Acute alcohol action and desensitization of ligand-gated ion channels. *Pharmacol Rev* **61**:98–114.

Eccles R (1994) Menthol and related cooling compounds. *J Pharm Pharmacol* **46**: 618–630.

Faerber L, Drechsler S, Ladenburger S, Gschaidmeier H, and Fischer W (2007) The neuronal 5-HT3 receptor network after 20 years of research—evolving concepts in management of pain and inflammation. *Eur J Pharmacol* **560**:1–8.

Fajardo O, Meseguer V, Belmonte C, and Viana F (2008) TRPA1 channels mediate cold temperature sensing in mammalian vagal sensory neurons: pharmacological and genetic evidence. *J Neurosci* **28**:7863–7875.

Farco JA and Grundmann O (2013) Menthol—pharmacology of an important naturally medicinal "cool". *Mini Rev Med Chem* **13**:124–131.

Galeotti N, Di Cesare Mannelli L, Mazzanti G, Bartolini A, and Ghelardini C (2002) Menthol: a natural analgesic compound. *Neurosci Lett* **322**:145–148.

Galligan JJ (2002) Ligand-gated ion channels in the enteric nervous system. *Neurogastroenterol Motil* **14**:611–623.

García DA, Bujons J, Vale C, and Suñol (2006) Allosteric positive interaction of thymol with the $GABA_A$ receptor in primary cultures of mouse cortical neurons. *Neuropharmacology* **50**:25–35.

Gaudioso C, Hao J, Martin-Eauclaire MF, Gabriac M, and Delmas P (2012) Menthol pain relief through cumulative inactivation of voltage-gated sodium channels. *Pain* **153**:473–484.

Gelal A, Jacob P, 3rd, Yu L, and Benowitz NL (1999) Disposition kinetics and effects of menthol. *Clin Pharmacol Ther* **66**:128–135.

Grigoleit HG and Grigoleit P (2005) Gastrointestinal clinical pharmacology of peppermint oil. *Phytomedicine* **12**:607–611.

Hall AC, Griffith TN, Tsikolia M, Kotey FO, Gill N, Humbert DJ, Watt EE, Yermolina YA, Goel S, and El-Ghendy B, et al. (2011) Cyclohexanol analogues are positive modulators of GABA(A) receptor currents and act as general anaesthetics in vivo. *Eur J Pharmacol* **667**:175–181.

Hall AC, Turcotte CM, Betts BA, Yeung WY, Agyeman AS, and Burk LA (2004) Modulation of human GABAA and glycine receptor currents by menthol and related monoterpenoids. *Eur J Pharmacol* **506**:9–16.

Haniadka R, Popouri S, Palatty PL, Arora R, and Baliga MS (2012) Medicinal plants as antiemetics in the treatment of cancer: a review. *Integr Cancer Ther* **11**:18–28.

Hans M, Wilhelm M, and Swandulla D (2012) Menthol suppresses nicotinic acetylcholine receptor functioning in sensory neurons via allosteric modulation. *Chem Senses* **37**:463–469.

Heimes K, Hauk F, and Verspohl EJ (2011) Mode of action of peppermint oil and (-)-menthol with respect to 5-HT3 receptor subtypes: binding studies, cation uptake by receptor channels and contraction of isolated rat ileum. *Phytother Res* **25**: 702–708.

Irwin JJ, Sterling T, Mysinger MM, Bolstad ES, and Coleman RG (2012) ZINC: a free tool to discover chemistry for biology. *J Chem Inf Model* **52**:1757–1768.

Jordt SE, McKemy DD, and Julius D (2003) Lessons from peppers and peppermint: the molecular logic of thermosensation. *Curr Opin Neurobiol* **13**:487–492.

Klasen K, Hollatz D, Zielke S, Gisselmann G, Hatt H, and Wetzel CH (2012) The TRPM8 ion channel comprises direct Gq protein-activating capacity. *Pflugers Arch* **463**:779–797.

Larkin MA, Blackshields G, Brown NP, Chenna R, McGettigan PA, McWilliam H, Valentin F, Wallace IM, Wilm A, and Lopez R, et al. (2007) Clustal W and Clustal X version 2.0. *Bioinformatics* **23**:2947–2948.

Lipinsky D and Oron Y (1996) Alkaline pH facilitates the exchange of guanine nucleotides: a possible mechanism for modulation of the kinetics of responses mediated by guanine nucleotide-binding proteins. *J Cell Physiol* **169**:167–174.

Lovinger DM and Zhou Q (1993) Trichloroethanol potentiation of 5-hydroxytryptamine3 receptor-mediated ion current in nodose ganglion neurons from the adult rat. *J Pharmacol Exp Ther* **265**:771–776.

Lu HF, Hsueh SC, Yu FS, Yang JS, Tang NY, Chen SC, and Chung JG (2006) The role of Ca^{2+} in (-)-menthol-induced human promyelocytic leukemia HL-60 cell death. *In Vivo* **20**:69–75.

Macpherson LJ, Hwang SW, Miyamoto T, Dubin AE, Patapoutian A, and Story GM (2006) More than cool: promiscuous relationships of menthol and other sensory compounds. *Mol Cell Neurosci* **32**:335–343.

McCool BA and Lovinger DM (1995) Ifenprodil inhibition of the 5-hydroxytryptamine3 receptor. *Neuropharmacology* **34**:621–629.

Miyazawa A, Fujiyoshi Y, and Unwin N (2003) Structure and gating mechanism of the acetylcholine receptor pore. *Nature* **423**:949–955.

Morris GM, Huey R, Lindstrom W, Sanner MF, Belew RK, Goodsell DS, and Olson AJ (2009) AutoDock4 and AutoDockTools4: automated docking with selective receptor flexibility. *J Comput Chem* **30**:2785–2791.

Namer B, Seifert F, Handwerker HO, and Maihöfner C (2005) TRPA1 and TRPM8 activation in humans: effects of cinnamaldehyde and menthol. *Neuroreport* **16**: 955–959.

Neumann JT and Copello JA (2011) Cross-reactivity of ryanodine receptors with plasma membrane ion channel modulators. *Mol Pharmacol* **80**:509–517.

Onaran HO and Costa T (2009) Allosteric coupling and conformational fluctuations in proteins. *Curr Protein Pept Sci* **10**:110–115.
Oz M (2006) Receptor-independent actions of cannabinoids on cell membranes: focus on endocannabinoids. *Pharmacol Ther* **111**:114–144.
Oz M, Soldatov NM, Melia MT, Abernethy DR, and Morad M (1998) Functional coupling of human L-type Ca2+ channel and angiotensin AT1A receptor coexpressed in Xenopus oocytes. *Mol Pharmacol* **54**:1106–1112.
Oz M, Spivak CE, and Lupica CR (2004a) The solubilizing detergents, Tween 80 and Triton X-100 non-competitively inhibit alpha 7-nicotinic acetylcholine receptor function in Xenopus oocytes. *J Neurosci Methods* **137**:167–173.
Oz M, Zakharova IO, Dinc M, and Shippenberg T (2004b) Cocaine inhibits cromakalim-activated K+ currents in follicle-enclosed Xenopus oocytes. *Naunyn Schmiedebergs Arch Pharmacol* **369**:252–259.
Oz M, Zhang L, and Morales M (2002a) Endogenous cannabinoid, anandamide, acts as a noncompetitive inhibitor on 5-HT3 receptor-mediated responses in Xenopus oocytes. *Synapse* **46**:150–156.
Oz M, Zhang L, Rotondo A, Sun H, and Morales M (2003) Direct activation by dopamine of recombinant human 5-HT1A receptors: comparison with human 5-HT2C and 5-HT3 receptors. *Synapse* **50**:303–313.
Oz M, Zhang L, and Spivak CE (2002b) Direct noncompetitive inhibition of 5-HT(3) receptor-mediated responses by forskolin and steroids. *Arch Biochem Biophys* **404**: 293–301.
Palade P (1987) Drug-induced Ca2+ release from isolated sarcoplasmic reticulum. II. Releases involving a Ca2+-induced Ca2+ release channel. *J Biol Chem* **262**: 6142–6148.
Pan R, Tian Y, Gao R, Li H, Zhao X, Barrett JE, and Hu H (2012) Central mechanisms of menthol-induced analgesia. *J Pharmacol Exp Ther* **343**:661–672.
Park TJ, Seo HK, Kang BJ, and Kim KT (2001) Noncompetitive inhibition by camphor of nicotinic acetylcholine receptors. *Biochem Pharmacol* **61**:787–793.
Patel T, Ishiuji Y, and Yosipovitch G (2007) Menthol: a refreshing look at this ancient compound. *J Am Acad Dermatol* **57**:873–878.
Priestley CM, Williamson EM, Wafford KA, and Sattelle DB (2003) Thymol, a constituent of thyme essential oil, is a positive allosteric modulator of human GABA (A) receptors and a homo-oligomeric GABA receptor from Drosophila melanogaster. *Br J Pharmacol* **140**:1363–1372.
Riering K, Rewerts C, and Zieglgänsberger W (2004) Analgesic effects of 5-HT3 receptor antagonists. *Scand J Rheumatol Suppl* **119**:19–23.
Roy A, Kucukural A, and Zhang Y (2010) I-TASSER: a unified platform for automated protein structure and function prediction. *Nat Protoc* **5**:725–738.
Rüsch D, Braun HA, Wulf H, Schuster A, and Raines DE (2007) Inhibition of human 5-HT(3A) and 5-HT(3AB) receptors by etomidate, propofol and pentobarbital. *Eur J Pharmacol* **573**:60–64.
Sanghvi M, Hamouda AK, Davis MI, Morton RA, Srivastava S, Pandhare A, Duddempudi PK, Machu TK, Lovinger DM, and Cohen JB, et al. (2009) Hydrophobic photolabeling studies identify the lipid-protein interface of the 5-HT3A receptor. *Biochemistry* **48**:9278–9286.
Sanner MF (1999) Python: a programming language for software integration and development. *J Mol Graph Model* **17**:57–61.
Sanner M, Stoffler D, and Olson AJ (2002) ViPEr, a visual programming environment for Python, in *Proceedings of the 10th International Python Conference*; 2002 February 4-7. pp 103–115.
Sherkheli MA, Vogt-Eisele AK, Bura D, Beltrán Márques LR, Gisselmann G, and Hatt H (2010) Characterization of selective TRPM8 ligands and their structure activity response (S.A.R) relationship. *J Pharm Pharm Sci* **13**:242–253.
Spivak CE, Lupica CR, and Oz M (2007) The endocannabinoid anandamide inhibits the function of α4β2 nicotinic acetylcholine receptors. *Mol Pharmacol* **72**:1024–1032.
Takeuchi S, Tamaoki J, Kondo M, and Konno K (1994) Effect of menthol on cytosolic Ca2+ levels in canine airway epithelium in culture. *Biochem Biophys Res Commun* **201**:1333–1338.
Thompson AJ, Lester HA, and Lummis SC (2010) The structural basis of function in Cys-loop receptors. *Q Rev Biophys* **43**:449–499.
Thompson AJ and Lummis SC (2007) The 5-HT3 receptor as a therapeutic target. *Expert Opin Ther Targets* **11**:527–540.
Trombetta D, Castelli F, Sarpietro MG, Venuti V, Cristani M, Daniele C, Saija A, Mazzanti G, and Bisignano G (2005) Mechanisms of antibacterial action of three monoterpenes. *Antimicrob Agents Chemother* **49**:2474–2478.
Turina AV, Nolan MV, Zygadlo JA, and Perillo MA (2006) Natural terpenes: self-assembly and membrane partitioning. *Biophys Chem* **122**:101–113.
Tsuzuki K, Xing H, Ling J, and Gu JG (2004) Menthol-induced Ca^{2+} release from presynaptic Ca^{2+} stores potentiates sensory synaptic transmission. *J Neurosci* **24**: 762–771.
Watt EE, Betts BA, Kotey FO, Humbert DJ, Griffith TN, Kelly EW, Veneskey KC, Gill N, Rowan KC, and Jenkins A, et al. (2008) Menthol shares general anesthetic activity and sites of action on the GABA(A) receptor with the intravenous agent, propofol. *Eur J Pharmacol* **590**:120–126.
Williams DB and Akabas MH (2002) Structural evidence that propofol stabilizes different GABA(A) receptor states at potentiating and activating concentrations. *J Neurosci* **22**:7417–7424.
Wright CE, Bowen WP, Grattan TJ, and Morice AH (1998) Identification of the L-menthol binding site in guinea-pig lung membranes. *Br J Pharmacol* **123**:481–486.
Yakel JL and Jackson MB (1988) 5-HT3 receptors mediate rapid responses in cultured hippocampus and a clonal cell line. *Neuron* **1**:615–621.
Yang KH, Galadari S, Isaev D, Petroianu G, Shippenberg TS, and Oz M (2010b) The nonpsychoactive cannabinoid cannabidiol inhibits 5-hydroxytryptamine3A receptor-mediated currents in Xenopus laevis oocytes. *J Pharmacol Exp Ther* **333**:547–554.
Yang KH, Isaev D, Morales M, Petroianu G, Galadari S, and Oz M (2010a) The effect of Δ9-tetrahydrocannabinol on 5-HT3 receptors depends on the current density. *Neuroscience* **171**:40–49.
Yosipovitch G, Szolar C, Hui XY, and Maibach H (1996) Effect of topically applied menthol on thermal, pain and itch sensations and biophysical properties of the skin. *Arch Dermatol Res* **288**:245–248.
Zhang X, Mak S, Li L, Parra A, Denlinger B, Belmonte C, and McNaughton PA (2012) Direct inhibition of the cold-activated TRPM8 ion channel by Gαq. *Nat Cell Biol* **14**: 851–858.
Zhang XB, Jiang P, Gong N, Hu XL, Fei D, Xiong ZQ, Xu L, and Xu TL (2008) A-type GABA receptor as a central target of TRPM8 agonist menthol. *PLoS ONE* **3**:e3386.
Zhang Y (2008) I-TASSER server for protein 3D structure prediction. *BMC Bioinformatics* **9**:40.
Zhang Y and Skolnick J (2005) TM-align: a protein structure alignment algorithm based on the TM-score. *Nucleic Acids Res* **33**:2302–2309.

Address correspondence to: Dr. Murat Oz, Laboratory of Functional Lipidomics, Department of Pharmacology and Therapeutics, College of Medicine and Health Sciences, UAE University, Al Ain, Ab 17666, United Arab Emirates. E-mail: Murat_Oz@uaeu.ac.ae